

---

GALLIUM ARSENIDE and  
RELATED COMPOUNDS 1974

---



# **Gallium Arsenide and related compounds, 1974**

Papers from the Fifth International Symposium on  
Gallium Arsenide and related compounds held in  
Deauville, 24-26 September 1974

**Conference Series Number 24**  
**The Institute of Physics**  
**London and Bristol**

---

DS56/08

Copyright © 1975 by The Institute of Physics and individual contributors. All rights reserved. Multiple copying of the contents or parts thereof without permission is in breach of copyright but permission is hereby given to copy titles and abstracts of papers and names of authors. Permission is usually given upon written application to the Institute to copy illustrations and short extracts from the text of individual contributions provided that the source (and, where appropriate, the copyright) is acknowledged.

ISBN 0 85498 114 4

ISSN 0 305 2346

The Fifth International Symposium on Gallium Arsenide and related compounds was jointly sponsored by The Institute of Physics, la Société Française de Physique, la Société des Electriciens, des Electroniciens et des Radioélectriciens and the United States Air Force Avionics Laboratory.

**International Organizing Committee**

J Bok (*France, Chairman*)

C Hilsum (*UK*)

R Runnels (*USA*)

H Strack (*Germany*)

R Veilex (*France, Secretary*)

**Honorary Editor**

J Bok

Published by The Institute of Physics, 47 Belgrave Square, London SW1X 8QX, England, and Techno House, Redcliffe Way, Bristol BS1 6NX, England, in association with the American Institute of Physics, 335 East 45th Street, New York, NY 10017, USA.

Set in 10/12 Press Roman, and printed in Great Britain by Adlard and Son Ltd, Dorking, Surrey.

## Preface

The impact of semiconductor devices on modern industry and even on everyday life is well known. Among all semiconductors, silicon has emerged as the only one to be used extensively at the moment. The success of this material is due to the fundamental knowledge of its physical properties, to the almost perfect control of its preparation, and to the device technology.

For many years gallium arsenide and the related III-V compounds have been actively studied for two reasons. Some of their properties allow important improvements on the performances of classical devices: higher mobilities and larger gaps, allowing higher frequency and temperature operation. Some characteristic features of III-V compounds give rise to new physical phenomena, such as high frequency electrical instabilities (Gunn effect) and light emission by carrier recombination.

These phenomena have recently been used in such types of devices as microwave oscillators and amplifiers, and light-emitting diodes and lasers. The future of these new compounds seems very promising especially for their application to optical telecommunications. This is the reason why physicists and metallurgists actively engaged in research on gallium arsenide and related compounds have met every two years since 1966 to discuss all aspects of device research and applications of the larger gap III-V compounds. The fifth international symposium of this series was held in Deauville, France, in September 1974. Two hundred and twenty participants attended: over ninety papers were submitted to the programme committee who had to select thirty six of these to be presented at the conference. Scientists from all the main universities, government or industrial laboratories throughout the world (with the exception of the Soviet Union), came to discuss the latest progress made on materials preparation, characterization and device technology. Topics discussed at the conference covered material analysis, crystal growth by liquid phase, vapour phase or molecular beam epitaxy, microwave devices, optoelectronic devices and light-emitting diodes, and device processing.

Some important progress was reported, the most significant being the large increase of operating life of (AlGa)As heterojunction lasers. It is well established that metallurgical factors are important in the control of gradual degradation of electroluminescent and laser diodes. New methods of processing and careful junction area definition give cw operating lifetimes of over 8000 hours. One of the conclusions of the conference is that there is definitely an industrial future for GaAs and related compounds in microwave and optical telecommunications.

Acknowledgments are due to our colleagues of the programme committee who were remarkably efficient in preparing the scientific programme and in selecting the papers presented at the conference, to the secretary of the meeting, Dr R Veilex, who took care of all the administration and to Dr J Lefèvre for local organization in Deauville.

It is my pleasure to thank our sponsors, the Délégation Générale à la Recherche Scientifique et Technique (DGRST), Ministère de l'Industrie et de la Recherche and the Direction de la Recherche et des Moyens d'Essais (DRME), Ministère de la Défense, for their financial support which made this conference possible.

J Bok

## Contents

### v Preface

#### Chapter 1:

##### Material preparation

- 1–9 Acceptor incorporation in GaAs grown by molecular beam epitaxy  
*M Ilegems and R Dingle*
- 10–15 Liquid phase epitaxy apparatus for thin layers and multiple layers  
*E Bauser, M Frik, K S Loechner and L Schmidt*
- 16–21 Growth of  $\text{In}_{1-x}\text{Ga}_x\text{Sb}$  by liquid phase epitaxy  
*H Miki, K Segawa, M Otsubo, K Shirahata and K Fujibayashi*
- 22–30 Vapour phase epitaxial growth of GaAs for multiple applications  
*L Hollan*
- 31–36 Diffusion limited LPE growth of InP layers for microwave devices  
*V L Wrick and L F Eastman*
- 37–45 New structures by liquid phase epitaxy for microwave devices  
*F E Rosztoczy, R E Goldwasser and J Kinoshita*

#### Chapter 2:

##### Microwave devices

- 46–54 Multi-layer epitaxial technology for the Schottky-barrier GaAs field-effect transistor  
*T Nozaki, M Ogawa, H Terao and H Watanabe*
  - 55–60 Schottky-barrier diodes fabricated on epitaxial GaAs using electron beam lithography  
*G T Wrixon and R F W Pease*
  - 61–70 Performance and characterization of X-band GaAs Read-type IMPATT diodes  
*F Hasegawa, Y Aono and Y Kaneko*
  - 71–76 High efficiency avalanche diodes from 10 to 15 GHz  
*A Farrrayre, B Kramer and A Mircea*
  - 77–88 New design criteria of Gunn diode contacts  
*T Sebestyen, H Hartnagel and L Herron*
-

- 89–93 Indium phosphide cw transferred electron amplifiers  
*F Corlett, I Griffith and J J Purcell*
- 94–101 Characteristics of  $\text{Ga}_x\text{In}_{1-x}\text{Sb}$  transferred-electron devices  
*J Michel, R Esquirol, A Jouillie and E Groubert*

### Chapter 3:

#### Optoelectronics: I. Material preparation

- 102–112 A comparison of  $\text{In}_x\text{Ga}_{1-x}\text{As}$ : Ge and GaAs: Si prepared by liquid phase epitaxy  
*M Ettenberg and H F Lockwood*
- 113–120 Growth and properties of  $\text{Ga}_y\text{Al}_{1-y}\text{As}-\text{Ga}_x\text{In}_{1-x}\text{P}$  heterostructure electroluminescent diodes  
*H Beneking, N Grote, P Mischel and G Schul*
- 121–133 The preparation and properties of bulk indium phosphide crystals and of indium phosphide light emitting diodes operating near  $1.05\text{ }\mu\text{m}$  wavelength  
*K J Bachmann, E Buehler, J L Shay and D L Malm*
- 134–144 Synthesis of GaP by gallium solution growth in a horizontal sealed ampoule  
*G Poiblaud and G Jacob*
- 145–154 A simple LPE process for efficient red and green GaP diodes  
*C Weyrich, G H Winstel, K Mettler and M Plihal*
- 155–164 Peltier-induced growth of GaAlAs  
*J J Daniele and C Michel*
- 165–173 Surface morphology in GaAs– $\text{Al}_x\text{Ga}_{1-x}\text{As}$  DH LPE layers  
*K K Shih, G R Woolhouse, A E Blakeslee and J M Blum*

### Chapter 4:

#### Optoelectronics: II. Devices

- 174–180 Degradation of GaAs–(Al,Ga)As double heterostructure light-emitting diodes  
*K Ikeda, T Tanaka, M Ishii and A Ito*
- 181–191 Characterization of GaAs–AlGaAs double-heterojunction laser structures using optical excitation  
*G A Acket, W Nijman, R P Tijburg and P J de Waard*
- 192–199 (AlGa)As double heterojunction cw lasers: the effect of device fabrication parameters on reliability  
*I Ladany and H Kressel*
- 200–209 Devices based on electroabsorption effects in reverse-biased GaAs–GaAlAs double heterostructures  
*J C Dymont, F P Kapron and A J SpringThorpe*

- 210–222 GaAs electroabsorption avalanche photodiode detectors  
*G E Stillman, C M Wolfe, J A Rossi and J L Ryan*
- 223–228 Phase diagram considerations of GaAs hetero-solar cells  
*D Huber and W Gramann*

**Chapter 5:**  
**Material analysis**

- 229–244 The incorporation of residual impurities in vapour grown GaAs  
*D J Ashen, P J Dean, D T J Hurle, J B Mullin, A Royle and A M White*
- 245–253 Diffusion length studies in n-gallium arsenide  
*A M Sekela, D L Feucht and A G Milnes*
- 254–265 On the oxygen donor concentration in GaP grown from a solution of GaP in Ga  
*R C Peters and A T Vink*
- 266–274 Photoemission and secondary emission of gallium phosphide epitaxial layers  
*C Piaget, P Guittard, J P Andre and P Saget*
- 275–291 Precision lattice parameter measurements on doped gallium arsenide  
*C M H Driscoll, A F W Willoughby, J B Mullin and B W Straughan*
- 292–306 Mobility, dopant and carrier distributions at the interface between semiconducting and semi-insulating gallium arsenide  
*K Lehovc and R Zuleeg*
- 307–319 Analysis of metal–GaAs Schottky-barrier diodes by secondary ion mass spectrometry  
*H B Kim, G G Sweeney and T M S Heng*

**Chapter 6:**  
**Device technology**

- 320–330 An electrochemical technique for automatic depth profiles of carrier concentration  
*T Ambridge and M M Faktor*
- 331–341 The ion implantation of donors for  $n^+$ –p junctions in GaAs  
*J M Woodcock and D J Clark*
- 342–354 Transport properties of  $O^+$  implanted in GaAs  
*M I Abdalla, J F Palmier and C Desfeux*

**Chapter 7:**  
**Special topics**

- 355–361 Automated Czochralski growth of III–V compounds  
*W Bardsley, G W Green, C H Holliday, D T J Hurle, G C Joyce, W R Macewan and P J Tufton*



- 362–368 An in-situ etch for the CVD growth of GaAs: the ‘He-etch’  
*J V DiLorenzo*
- 369–372 Nouvelle technique de croissance epitaxiale de InP  
*N Sol, J P Clariou, N T Linh, G Bichon and M Moulin*
- 373–376 A (GaAl)As–GaAs heterojunction structure for studying the role of the  
cathode contact on transferred electron devices  
*B W Clark, H G B Hicks, I G A Davies and J S Heeks*
- 377 Author Index

# Acceptor incorporation in GaAs grown by beam epitaxy

M Ilegems and R Dingle

Bell Laboratories, Murray Hill, New Jersey 07974, USA

**Abstract.** Undoped GaAs grown from Ga and As<sub>4</sub> beams is generally  $10^{15}$ – $10^{16}$  cm<sup>-3</sup> p-type with mobilities in the range 380–400 cm<sup>2</sup> V<sup>-1</sup> s<sup>-1</sup> (296 K) and 4200–5100 cm<sup>2</sup> V<sup>-1</sup> s<sup>-1</sup> (77 K). C (27 meV) and Mn (113 meV) are identified as persistent residual acceptors by low-temperature photoluminescence and Hall measurements. Under Ga-rich growth conditions the concentration of C acceptors (on As sites) increases, while the concentration of Mn acceptors (on Ga sites) decreases. These observations are consistent with reduced As-coverage of the growth surface and parallel the behaviour previously reported for Ge. Under As-rich growth conditions 296 K hole concentrations up to about  $1 \times 10^{18}$  cm<sup>-3</sup> may be achieved with Mn doping at a growth temperature of about 580 °C and with surface morphology equivalent to that obtained in undoped layers.

## 1. Introduction

Incorporation of dopants in GaAs grown by molecular beam epitaxy (MBE) is quite different from that in material grown by the more usual liquid phase epitaxy (LPE) or chemical vapour deposition (CVD) techniques. The difference is especially marked for the p-type dopants. Thus the traditional group II dopants, Zn and Cd, are very difficult to incorporate during MBE growth because of their high vapour pressures and concomitant low sticking probabilities to the growth surface, whereas the amphoteric group IV dopants Si, Ge and Sn are incorporated predominantly as donors on Ga sites under the usual MBE growth conditions.

Serious efforts are presently being made to exploit the unique capabilities of MBE for device applications and fundamental studies. Among the most significant recent advances in this respect are the demonstration by Cho and Casey (1974) of pulsed lasing action in AlGaAs–GaAs–AlGaAs double heterostructure lasers and the observation by Dingle *et al* (1974) of quantum effects in extremely thin AlGaAs–GaAs–AlGaAs heterostructures.

In view of the emerging device applications it is increasingly important to study impurity incorporation and basic material parameters in further detail. In this context, we report in the present paper first, on the nature of the residual impurities in beam epitaxial GaAs and their incorporation under different growth conditions, and secondly, on the use of Mn as a possible dopant for achieving high-conductivity p-type layers with beam epitaxy.

## 2. Crystal growth

Crystals from two different growth systems were studied. The growth configuration is similar to that described by Cho (1971) and a schematic cross-section of one of the

5504783

systems used is illustrated in figure 1. The apparatus consists essentially of an ion pumped high-vacuum station which contains a substrate mounted on a heating block and several individually heated pyrolytic BN evaporation cells enclosed in a liquid-nitrogen cooled shroud which serves to collimate the beams from the ovens as well as to pump condensible gases. The associated instrumentation includes a quadrupole mass spectrometer for

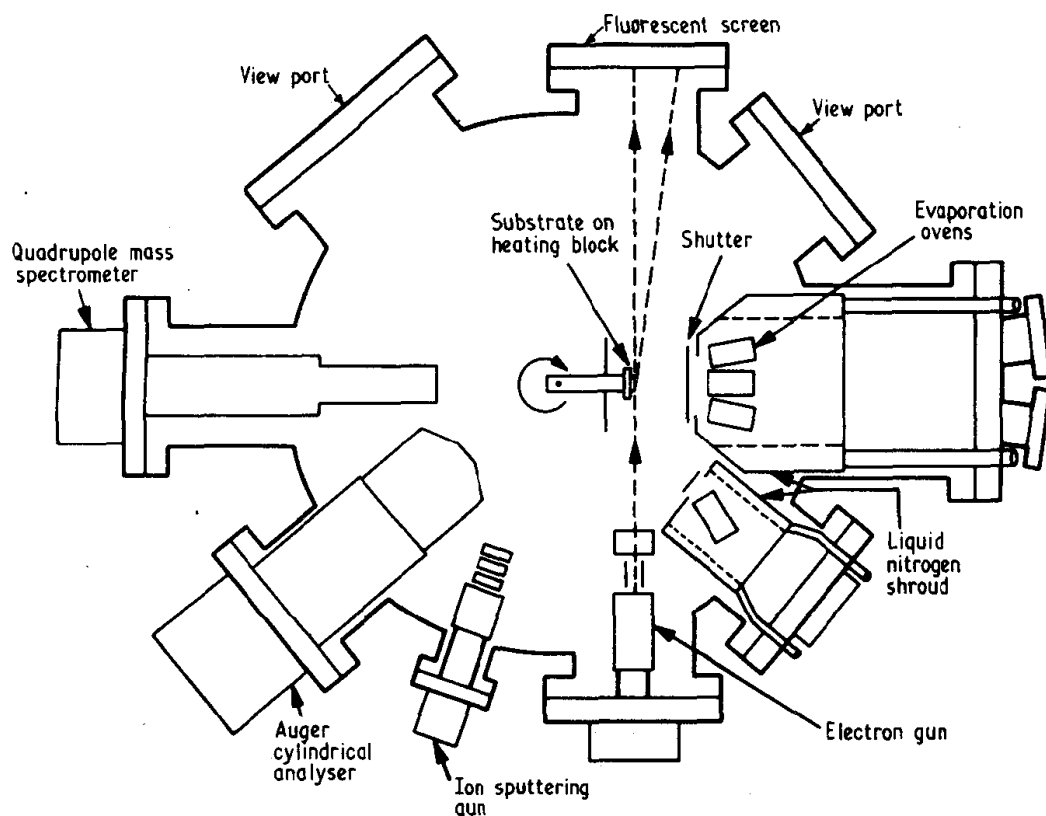


Figure 1. Cross-section of vacuum deposition system.

monitoring the molecular-beam constituents and background gases in the system, an Auger spectrometer for analysis of the chemical composition of the surface and a 3–5 kV electron gun for the observation of surface structures by glancing-incidence electron diffraction during growth.

Layers were grown on (100)-oriented Cr-doped GaAs substrates which had been chemically polished in bromine-methanol and cleaned *in situ* by ion sputtering. Substrate temperatures were maintained in the range of 560–600 °C during epitaxial deposition and growth rates were generally around  $1 \mu\text{m h}^{-1}$ . Elemental  $\alpha$ -As and Ga, both with nominal total impurity concentrations below  $1 \times 10^{-6}$  (mole fraction) were used as source materials.

Oven temperatures during growth are about 900 °C for Ga and about 300 °C for As with  $\text{As}_4$  as the dominant species effusing from the As oven. Temperatures are measured with chromel–alumel thermocouples embedded in a graphite slug which either supports the crucible or, for more accurate measurements, is placed at the bottom of the crucible in direct contact with the melt. Background pressures prior to growth are in the low

$10^{-9}$  Torr range. During growth the system pressure is around  $2 \times 10^{-7}$  Torr and is due mainly to  $\text{As}_4$ .

### 3. As-rich versus Ga-rich growth conditions

At any given substrate temperature a minimum As-flux is needed to maintain the so-called (Cho 1970) As-stabilized surface structure. This minimum flux corresponds to the equilibrium vapour pressure of As over a stoichiometric GaAs surface at that temperature.

When the substrate is heated in vacuum prior to growth, the amount of As evaporating from the surface will initially exceed that of Ga so that the surface of the crystal becomes depleted in As or Ga-rich (Arthur 1974). The electron diffraction pattern obtained under these conditions has been referred to by Cho (1970) as originating from a Ga-stabilized surface. Since under these conditions the surface and the bulk are of different composition, one would expect that the Ga-stabilized surface structure will be very difficult to maintain during growth except perhaps at very low growth rates. In practice, when the As/Ga flux ratio during growth is below that required to maintain an As-rich condition, excess Ga will build up at the surface. In extreme cases droplets of Ga appear, while under only slight excess-Ga conditions the growth surface remains smooth and mirror-like but shows a characteristic haziness. The properties of layers grown under these conditions may be expected to approach those of crystals grown by LPE. Our results, discussed below, substantiate this expectation.

When the As/Ga flux ratio is larger than that required to grow stoichiometric GaAs, the excess As simply evaporates from the surface. Structurally perfect layers can thus be grown under a wide range of As fluxes. However, one may expect that the As pressure during growth will influence both impurity incorporation and native defect concentrations, and hence the electrical and optical properties of the layers.

## 4. Residual impurities in GaAs

### 4.1. Luminescence

Comparison of the low-temperature luminescence spectra of non-intentionally doped MBE films with those observed in very detailed studies of high-purity CVD and LPE layers, summarized by Dean (1974), leads to the identification of C, Si, and Ge as residual impurities. Luminescence spectra of two not advertently doped crystals grown in the same system and under similar conditions except for the As/Ga flux ratio are shown in figure 2. The bands marked C, Si, and Ge, arise from donor-acceptor (DA) and free electron-bound hole (BA) recombination involving unidentified shallow ( $\sim 6$  meV) donors and respectively a carbon ( $\sim 27$  meV), silicon ( $\sim 35$  meV) and germanium ( $\sim 41$  meV) acceptor. The higher energy features relate to free exciton (1.515 eV), exciton-donor (1.5138 eV), and exciton-acceptor (1.5120 eV) processes. Finally, the characteristic feature near 1.407 eV, previously observed in MBE crystals by Cho and Hayashi (1971a), is attributed to the presence of approximately 113 meV deep manganese acceptors.

There are several characteristic differences between the spectra of crystals grown under respectively Ga-rich and As-rich conditions. First, we find that in crystals grown

under Ga-rich conditions the exciton region (1.515–1.511 eV) is dominated by the strong sharp structure near 1.5120 eV which has been previously identified with excitons decaying at neutral acceptors. In these crystals one sees only very weak evidence for excitons decaying at neutral donor sites. In the corresponding As-rich crystals the inverse situation is observed with dominating neutral donor–exciton recombination at 1.5138 eV and very weak or no acceptor–exciton emission at 1.5120 eV. These observations demonstrate that growth under Ga-rich conditions leads to an increased incorporation of amphoteric dopants on acceptor (As) sites, and are consistent with the Ge-doping results of Cho and Hayashi (1971b). Secondly, the 1.407 eV spectrum, which we associate with an isolated manganese acceptor on a Ga site, is quite strong in crystals grown under As-rich conditions but invariably much weaker in layers grown under Ga-rich conditions. Again this is consistent with the conclusion that growth under Ga-rich conditions favours the incorporation of impurities on As-sites.

Of the four elements, C, Si, Ge, and Mn, only C should be considered as a residual impurity generally associated with the MBE growth process. In the spectra of figure 2 we attribute the presence of Si and Ge to contamination resulting from previous evaporation of these elements in the system, while the Mn is believed to originate from inadvertent heating of the stainless steel rods that support the evaporation ovens. Crystals grown subsequently in a newly assembled growth system in which molybdenum rods were used to support the ovens showed only carbon associated features. For the present discussion, however, we choose to show spectra from a weakly contaminated system which most clearly illustrate the effects of changing growth conditions.

The identification of the bands labelled C in figure 2 with BA and DA pair transitions

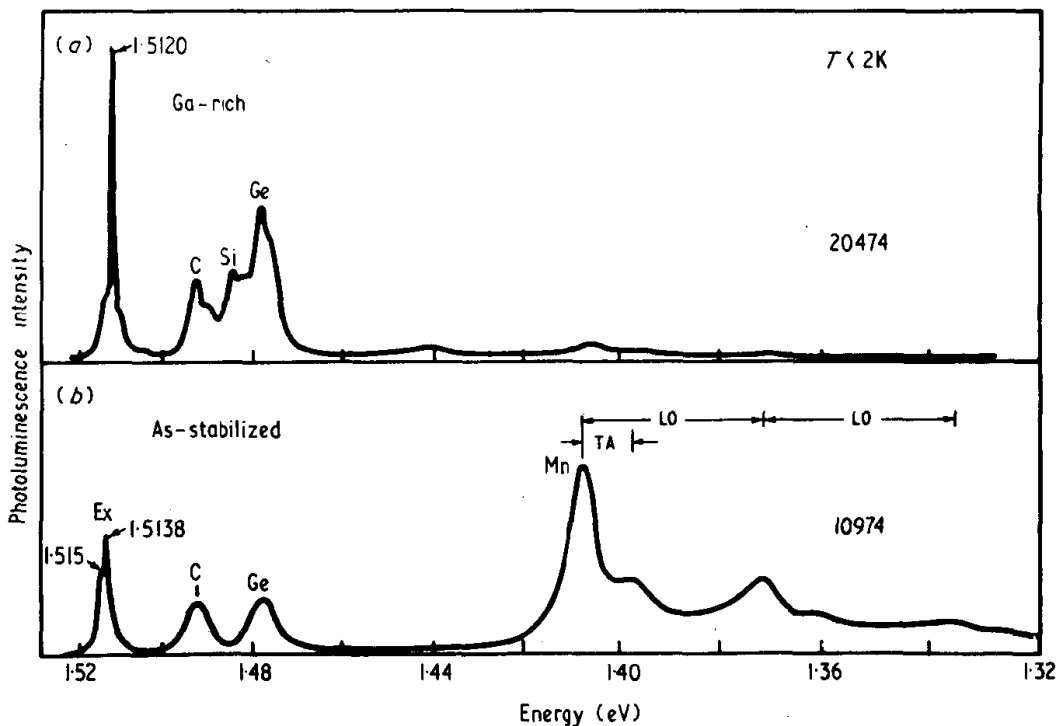


**Figure 2.** Photoluminescence of nominally undoped GaAs films grown under Ga-rich (a) or As-rich (b) conditions.

involving carbon acceptors is based on a comparison with the ionization energy for C reported by Dean (1974). In addition, we have also been able, in some cases, to resolve the characteristic ( $\sim 0.2$  meV) doublet splitting of the exciton peak at approximately 1.5120 eV. The presence of carbon in the grown layers is consistent with the fact that carbon is systematically detected by Auger analysis as a contaminant on initially clean GaAs surfaces after long exposure to the vacuum ambient.

Preliminary attempts were made to increase the concentration of C in the crystals by deliberate introductions of CO and C<sub>2</sub>H<sub>4</sub> in the growth zone during deposition. These experiments proved inconclusive as only rather weak increases in the strength of the pair and exciton transitions involving C relative to that of the other spectral features was observed. In addition no change in the electrical behaviour of the layers was apparent. The result is not unexpected in view of the very low sticking coefficients of CO and C<sub>2</sub>H<sub>4</sub> on GaAs at the growth temperature. The precise source of carbon contamination during growth is therefore still unidentified.

#### 4.2. Electrical properties

Undoped layers grown from elemental As and Ga sources are generally p-type. This is in contrast with the results reported (Cho 1971) for films grown using undoped GaAs as a source for As where the residual conductivity is n-type, presumably as a result of Si contamination originating from the GaAs source. We find residual room temperature hole concentrations from about  $1 \times 10^{15}$  to about  $1 \times 10^{16} \text{ cm}^{-3}$ . In one growth system and for crystals grown under As-rich conditions the p-type conductivity is invariably controlled by a deep acceptor at about 110 meV which we associate with the presence of Mn in the layers. In another growth system Mn is present in the crystals at much lower levels and the Hall data do not show the 110 meV controlled freeze-out at low temperatures. Plots of carrier concentration  $p = (eR_H)^{-1}$  and mobilities  $\mu_h = R_H/\rho$  against temperature are shown in figures 3 and 4 for two nominally undoped samples that are typical of the two growth systems. Where indicated the Hall curves have been fitted with the usual one acceptor-level expression:

$$p(p + N_D)/(N_A - N_D - p) = (m^*/g) \exp(-E_A/kT)$$

using the parameters listed in the figures.

In both 'undoped' samples of figure 3, as well as in all other undoped crystals measured, the carrier type changes from p to n at temperatures in the range from 100 to 200 °C. This transition to n-type suggests the presence of a moderately deep and presently unidentified electron trap. All data reported here have been limited to the temperature range where the influence of two carrier effects on the transport properties can be neglected.

The acceptor ionization energy  $E_A = 97$  meV deduced from the fit to the Hall data in figure 3 corresponds closely to the binding energy of the centre responsible for the deep 1.407 eV band observed in luminescence of crystals from the same growth system. This supports the DA origin of the 1.407 eV band observed in luminescence. In crystal 61273 which does not show the characteristic freeze-out the Hall data suggest the presence of a shallower level with energy around 30 meV, consistent with the presence of C in these crystals.

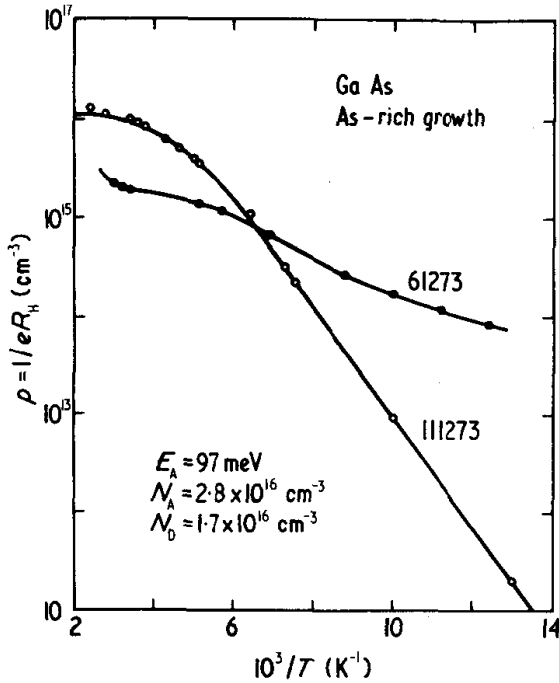


Figure 3. Hole concentration as a function of  $1/T$  for crystals from a Mn-contaminated (111273) or uncontaminated (61273) system.

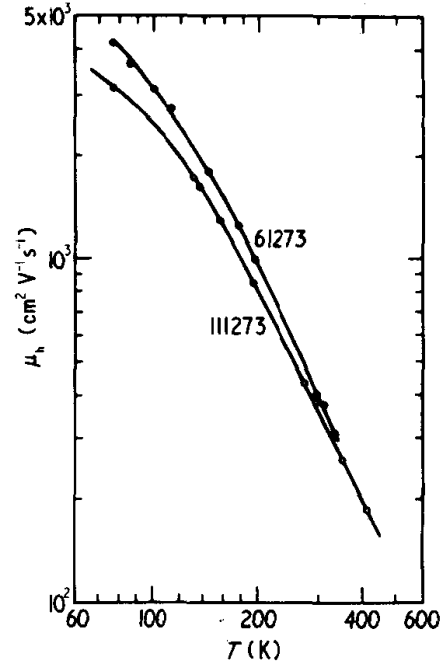


Figure 4. Mobility as a function of  $T$  for samples of figure 4.

The temperature dependence of the mobility shown in figure 4 for the same crystals as in figure 3 is typical of good-quality GaAs. The highest 77 K mobility measured in crystals grown under As-rich conditions is  $4200 \text{ cm}^2 \text{ V}^{-1} \text{ s}^{-1}$ ; for comparison the highest 77 K mobility reported to date for high purity  $p \sim 6 \times 10^{13} \text{ cm}^{-3}$  GaAs by Zschauer (1973) is  $9700 \text{ cm}^2 \text{ V}^{-1} \text{ s}^{-1}$ .

Electrical measurements confirm the dependence of Mn-acceptor incorporation upon the As/Ga ratio as observed in luminescence. Clear evidence of this is given in figure 5 where we compare two crystals grown in successive runs in the same system and under identical conditions except for a change in As-flux. The As-rich sample shows the usual dominance of the Mn-acceptor typical for this growth system. The Ga-rich crystal on the other hand shows essentially no carrier freeze-out associated with the acceptor level at about 113 meV. Mobilities of the Ga-rich crystals are generally slightly higher than those of the As-rich samples and their temperature dependence follows the behaviour shown in figure 4.

## 5. Mn doping

The initial identification of Mn as the impurity responsible for the 113 meV deep luminescence band and the corresponding carrier freeze out was based on the similarity between the luminescent spectra of the present crystals and those reported for Mn-diffused (Lee and Anderson 1964) samples as well as by comparison with the known activation energy for Mn (Vieland 1962). Other possibilities were considered, including the notion that a Ga-vacancy defect might be involved as was originally suggested by Cho and Hayashi (1971a). The difference observed between samples from different

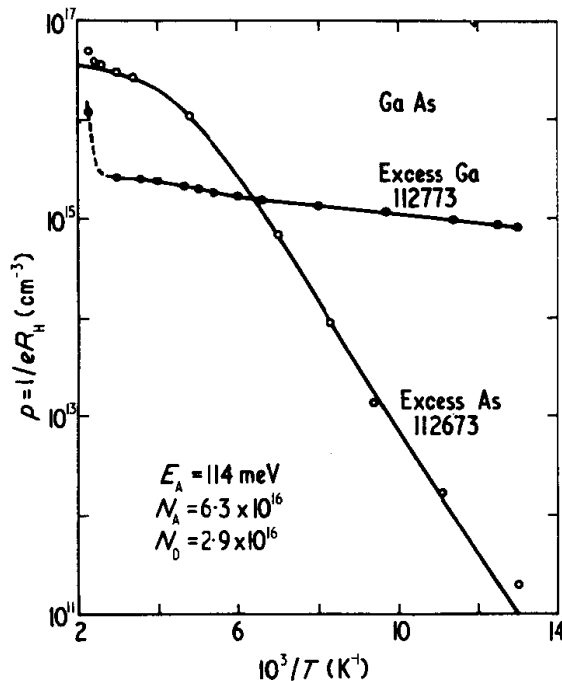


**Figure 5.** Hole concentration as a function of  $1/T$  for crystals grown in successive runs and under identical conditions except for a change in the As/Ga flux ratio.

growth systems however argues convincingly against a simple vacancy assignment although some forms of intrinsic defect–impurity complex cannot be ruled out on that basis.

The variation of the shape and intensity of the 1.407 eV luminescence band with excitation energy is consistent with the behaviour expected for transitions involving a deep isolated acceptor. Figure 6 shows how the high energy band of the spectrum resolves into several components as the excitation energy is reduced and gives evidence for the participation of conduction band–acceptor (1.4065 eV) and donor–acceptor

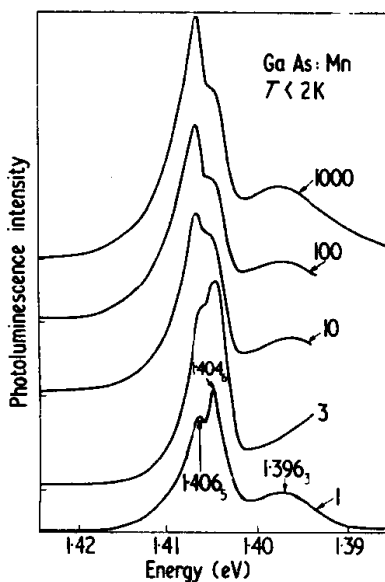


**Figure 6.** Photoluminescence of Mn-associated feature as a function of excitation level.



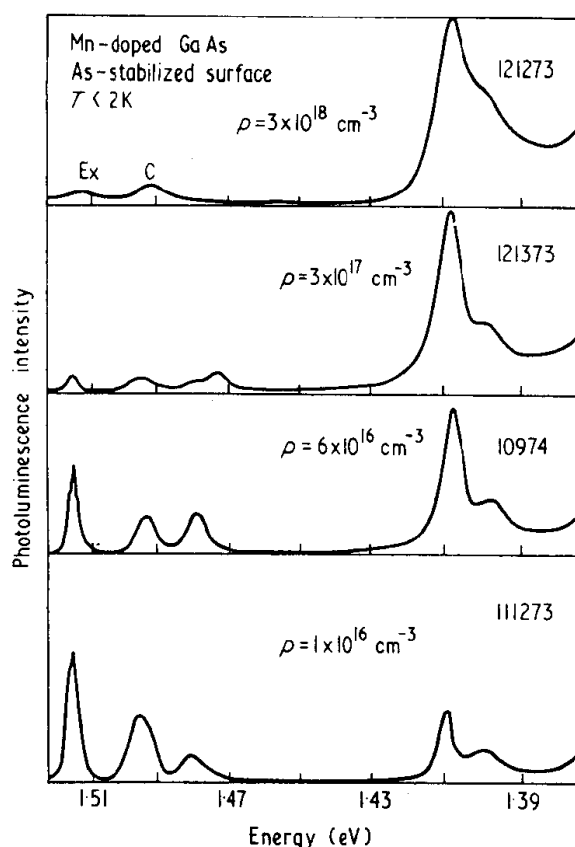


Figure 7. Photoluminescence of Mn-doped GaAs layers arranged in order of increasing doping level.

pair (1.4046 eV) recombination. The analysis of these data results in an acceptor binding energy of  $112.7 \pm 0.5$  meV.

In order to further characterize the Mn-acceptor as well as to investigate its possible use for p-type doping as an alternative to the use of Mg (Cho and Panish 1972) a number of growth runs were made using elemental Mn as a dopant. For all runs made under As-rich conditions, hole concentrations and 1.407 eV luminescence band intensities increased with increasing Mn addition. The luminescence results are illustrated in figure 7 for four layers with 296 K hole concentrations ranging from  $1 \times 10^{16} \text{ cm}^{-3}$  to  $3 \times 10^{18} \text{ cm}^{-3}$ . For crystals grown under Ga-rich conditions the Mn-associated luminescence remained very weak throughout.

The highest 296 K carrier concentration that could be achieved without affecting the growth morphology was  $p \approx 1 \times 10^{18} \text{ cm}^{-3}$  in the present system. For higher Mn fluxes the surface appearance deteriorated rapidly. It is not clear whether the limit at approximately  $1 \times 10^{18} \text{ cm}^{-3}$  represents the maximum solubility of Mn at the growth temperature of about 580 °C or whether the relatively high Mn flux interferes with the growth process. Hole activation energies in the Mn-doped crystals decrease with increasing doping levels above the  $10^{17} \text{ cm}^{-3}$  range, consistent with the results reported by Blakemore *et al* (1973). Room temperature mobilities measured for crystals with  $p = 2 \times 10^{17} \text{ cm}^{-3}$  and  $1.2 \times 10^{18} \text{ cm}^{-3}$  are 270 and  $180 \text{ cm}^2 \text{ V}^{-1} \text{ s}^{-1}$  respectively, as compared to mobilities in the range 380–400  $\text{cm}^2 \text{ V}^{-1} \text{ s}^{-1}$  found in undoped crystals (figure 4).